A galloping quadruped model using left–right asymmetry in touchdown angles

Masayasu Tanase[a], Yuichi Ambe[a], Shinya Aoi[b,c,*], Fumitoshi Matsuno[a]

[a] *Dept. of Mechanical Engineering and Science, Graduate School of Engineering, Kyoto University, Kyoto Daigaku-Katsura, Nishikyo-ku, Kyoto 615-8540, Japan*
[b] *Dept. of Aeronautics and Astronautics, Graduate School of Engineering, Kyoto University, Kyoto Daigaku-Katsura, Nishikyo-ku, Kyoto 615-8540, Japan*
[c] *JST, CREST, 5 Sanbancho, Chiyoda-ku, Tokyo 102-0075, Japan*

Abstract

Among quadrupedal gaits, the galloping gait has specific characteristics in terms of locomotor behavior. In particular, it shows a left–right asymmetry in gait parameters such as touchdown angle and the relative phase of limb movements. In addition, asymmetric gait parameters show a characteristic dependence on locomotion speed. There are two types of galloping gaits in quadruped animals: the transverse gallop, often observed in horses; and the rotary gallop, often observed in dogs and cheetahs. These two gaits have different footfall sequences. Although these specific characteristics in quadrupedal galloping gaits have been observed and described in detail, the underlying mechanisms remain unclear. In this paper, we use a simple physical model with a rigid body and four massless springs and incorporate the left–right asymmetry of touchdown angles. Our simulation results show that our model produces stable galloping gaits for certain combinations of model parameters and explains these specific characteristics observed in the quadrupedal galloping gait. The results are then evaluated in comparison with the measured data of quadruped animals and the gait mechanisms are clarified from the viewpoint of dynamics, such as the roles of the left–right touchdown angle difference in the generation of galloping gaits and energy transfer during one gait cycle to produce two different galloping

*Corresponding author
Email address: shinya_aoi@kuaero.kyoto-u.ac.jp (Shinya Aoi)

gaits.

Keywords: Galloping gait, Quadruped, Model, Touchdown angle, Left–right asymmetry, Center of mass movement, Energy transfer

1. Introduction

Quadruped animals use various gaits depending on the locomotion speed. They use a walking gait in the lowest range of locomotion speed, and this changes to a trotting gait as the locomotion speed increases. In the highest range of locomotion speed, they use a galloping gait. These gaits are characterized by footfall sequence [32]. During gaits used at slow speeds, such as a walking gait, at least one limb is in contact with the ground, that is, in the stance phase. In contrast, gaits used at higher speeds, such as a galloping gait, have a flight phase during which all four limbs are in the air, that is, in the swing phase. These gaits have been investigated from mechanical, energetic, kinematic, and kinetic viewpoints to clarify the underlying mechanism for the use of such different gaits depending on the locomotion speed [1, 13, 22, 23, 24, 31].

Among these quadrupedal gaits, the galloping gait has characteristic properties. Differing from the walking and trotting gaits, the galloping gait is asymmetric [1, 22, 23]. More specifically, the relative phase of the movements between the left and right limbs is away from the antiphase, unlike the walking and trotting gaits, as shown in Fig. 1**A**. In addition, as the locomotion speed increases, the relative phase decreases and approaches the in-phase as in a bounding gait, which is not generally used by large, cursorial quadrupeds [26]. There are two types of galloping gaits in quadruped animals, the transverse gallop and the rotary gallop, and the two gaits have different footfall sequences (Fig. 1**B**) [22]. The transverse gallop is the preferred gait of horses, and the foot contacts take place in the order of a hindlimb, the contralateral hindlimb, the ipsilateral forelimb, and the contralateral forelimb. The rotary gallop is the preferred gait of dogs and cheetahs, and the foot contacts occur in the sequence of a hindlimb, the

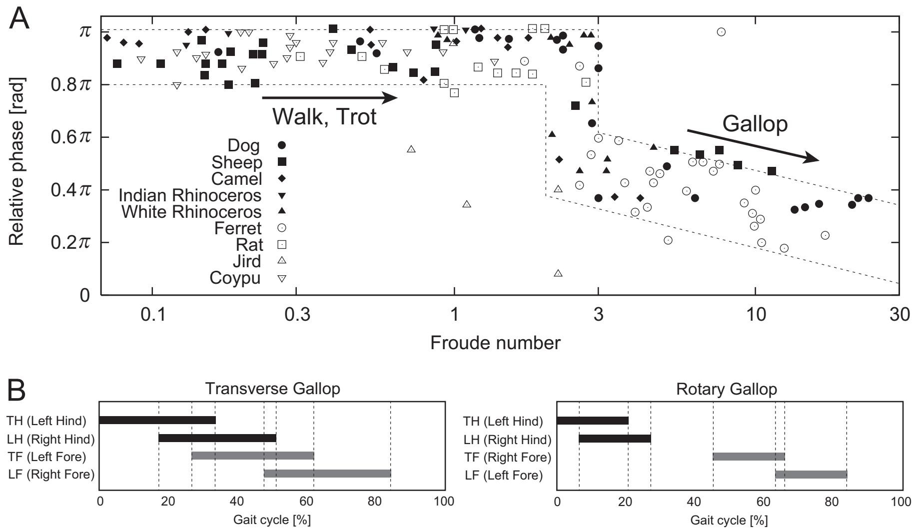

Figure 1: Characteristics of the quadrupedal galloping gait. **A**: relative phase between left and right forelimbs of quadrupeds depending on locomotion speed (Froude number), modified from [1]. Although it remains almost antiphase in the walking and trotting gaits, it is away from the antiphase and approaches the in-phase in the galloping gait as the locomotion speed increases. **B**: footfall diagrams of the transverse gallop of horses and the rotary gallop of dogs and cheetahs, modified from [22]. The transverse gallop has a single flight phase after the liftoff of the forelimbs, while the rotary gallop has two flight phases after the liftoff of the hindlimbs and forelimbs. TH: trailing hindlimb, TF: trailing forelimb, LH: leading hindlimb, and LF: leading forelimb.

contralateral hindlimb, the contralateral forelimb, and the ipsilateral forelimb. Both gallops have a flight phase after the liftoff of the forelimbs. In contrast, the fast rotary gallop of dogs and cheetahs has another flight phase after the liftoff of the hindlimbs, unlike the transverse gallop of horses [5, 23] (some species show a rotary gallop with just one flight phase at low speeds [25]). Although these specific characteristics in quadrupedal galloping gaits and the dependence on the locomotion speed and species have been observed and described in detail [1, 5, 22, 23], the underlying dynamic mechanisms remain unclear.

Locomotion in humans and animals involves moving the center of mass (COM) of the whole body using the limbs. The essential contribution of a limb in locomotion dynamics can be represented by a spring. To explain the locomotion mechanisms from a dynamic viewpoint, spring-loaded inverted pendulum models have been used [6, 7, 8, 9, 11, 16, 29, 30, 36]. In particular, for human running, the dependence of stability on touchdown angles has been clarified [17, 19, 38]. A simple model having mass and two springs has been used to explain the characteristic difference between human walking and running, which appears in the vertical ground reaction forces: a double-peaked shape in human walking, and a single-peaked shape in human running [18]. For quadrupedal locomotion, a rigid body with two springy legs has shown the stability characteristics of a bounding gait [10, 35]. The difference in the energy levels between the trotting, bounding, and galloping gaits also has been examined [33]. Although simple physical models with leg springs have been used for the quadrupedal galloping gait [21, 26, 28, 33, 40], they do not explain the above-mentioned specific characteristics. In this paper, we use a simple physical model with a rigid body and four massless springs. The simulation results show that our model produces stable galloping gaits for certain combinations of model parameters, and explains these specific characteristics in the quadrupedal galloping gait. The results are then evaluated in comparison with quadruped animals and the gait mechanisms are discussed from the viewpoint of dynamics.

2. Materials and Methods

2.1. Physical model

In this paper we use a physical model, which consists of a rigid body and four massless springs in two dimensions (Fig. 2), as used in [33]. x and y are, respectively, the horizontal and vertical positions of the COM of the body, and θ is the pitch angle. m and I are, respectively, the mass and moment of inertia around the COM. l is the distance between the COM and the root of the spring. g is the gravitational acceleration. $+x$ is the locomotion direction. The front two springs and the rear two springs represent the forelimbs and hindlimbs, respectively. The spring constant is k. In the forelimbs, the anterior limb during

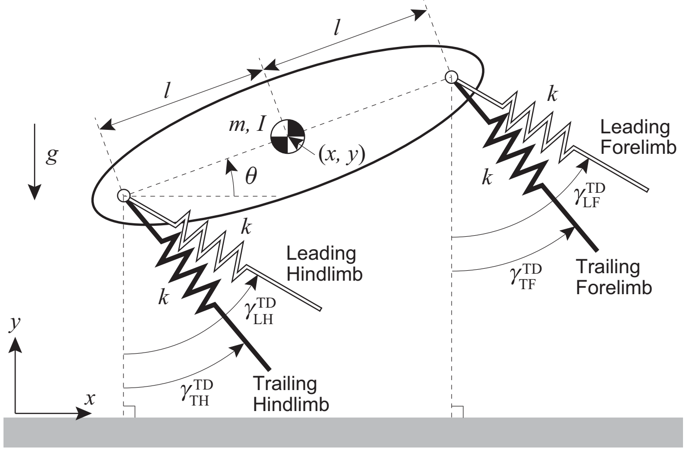

Figure 2: Physical model of galloping consisting of a rigid body and four massless springs in two dimensions.

the swing phase is the leading forelimb (LF) and the posterior limb is the trailing forelimb (TF). Similarly, the anterior and posterior hindlimbs during the swing phase are the leading hindlimb (LH) and trailing hindlimb (TH), respectively.

During the swing phase, the spring length remains the neutral length l_0 and the angle relative to the vertical line keeps the specific value γ_i^{TD} (i =LF, TF, LH, TH), which corresponds to the touchdown angle ($\gamma_{\mathrm{LF}}^{\mathrm{TD}} \geq \gamma_{\mathrm{TF}}^{\mathrm{TD}}$, $\gamma_{\mathrm{LH}}^{\mathrm{TD}} \geq \gamma_{\mathrm{TH}}^{\mathrm{TD}}$). We assumed $\gamma_{\mathrm{LF}}^{\mathrm{TD}} + \gamma_{\mathrm{TF}}^{\mathrm{TD}} \geq 0$ and $\gamma_{\mathrm{LH}}^{\mathrm{TD}} + \gamma_{\mathrm{TH}}^{\mathrm{TD}} \geq 0$ so that the trailing limbs contact the ground earlier than the leading limbs, as observed in quadruped animals. When a spring tip reaches the ground, it is constrained on the ground and behaves as a frictionless pin joint. When the spring length returns to the neutral length after the compression, the tip leaves the ground. Because the touchdown and liftoff occur at the neutral length, this physical system is energy conservative.

2.2. Governing equations

In our model, the four limbs have no influence on body dynamics during the swing phase. In contrast, during the stance phase, they work as springs and influence body dynamics through their compression. The motion of our model is governed by the equations of motion of x, y, and θ, which are given by

$$\begin{aligned}
m\ddot{x} &= \sum_{i=\mathrm{LF,TF,LH,TH}} -f_i \sin\gamma_i \\
m\ddot{y} &= \sum_{i=\mathrm{LF,TF,LH,TH}} f_i \cos\gamma_i - mg \\
I\ddot{\theta} &= \sum_{i=\mathrm{LF,TF}} f_i l \cos(\gamma_i - \theta) - \sum_{i=\mathrm{LH,TH}} f_i l \cos(\gamma_i - \theta)
\end{aligned} \tag{1}$$

where

$$f_i = \begin{cases} -k(l_i - l_0) & \text{stance phase} \\ 0 & \text{swing phase} \end{cases}$$

l_i and γ_i (i =LF, TF, LH, TH) are the spring length and the angle relative to the vertical line, respectively, which are determined by x, y, θ, l, and the touchdown position ($l_i = l_0$ and $\gamma_i = \gamma_i^{\mathrm{TD}}$ during the swing phase).

By using m, l_0, and $\sqrt{l_0/g}$ as the characteristic mass, length, and time scale of our model, the state variables and parameters become dimensionless as $x^* = x/l_0$, $y^* = y/l_0$, $\dot{()}^* = \dot{()}\sqrt{l_0/g}$, $I^* = I/(ml_0^2)$, $k^* = kl_0/(mg)$, $l^* = l/l_0$, and $l_i^* = l_i/l_0$, which yields the dimensionless equations of (1) by

$$\begin{aligned}
\ddot{x}^* &= \sum_{i=\mathrm{LF,TF,LH,TH}} -f_i^* \sin\gamma_i \\
\ddot{y}^* &= \sum_{i=\mathrm{LF,TF,LH,TH}} f_i^* \cos\gamma_i - 1 \\
I^*\ddot{\theta}^* &= \sum_{i=\mathrm{LF,TF}} f_i^* l^* \cos(\gamma_i - \theta) - \sum_{i=\mathrm{LH,TH}} f_i^* l^* \cos(\gamma_i - \theta)
\end{aligned} \tag{2}$$

where

$$f_i^* = \begin{cases} -k^*(l_i^* - 1) & \text{stance phase} \\ 0 & \text{swing phase} \end{cases}$$

2.3. Generation of galloping gait using the left–right asymmetry of touchdown angles

An important function of limbs in locomotion dynamics is to produce translational and rotational forces for the whole body through interaction with the

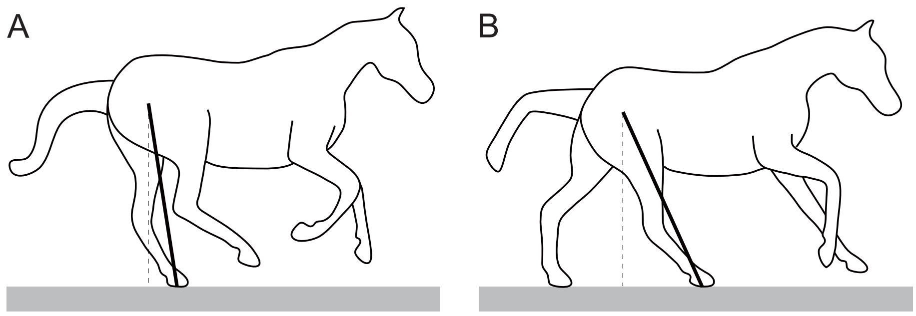

Figure 3: Different touchdown angles of (**A**) trailing and (**B**) leading hindlimbs in the horse galloping gait.

ground. Such forces are generated through the movements of the limb tip relative to the limb root (length and orientation). During a steady gait, the limb tip produces a periodic trajectory relative to the body. When the relative phase between the left and right limb movements is antiphase, as in walking and trotting gaits, the left and right limbs move alternately relative to the body and the periodic trajectories are almost identical between the left and right limbs. When the relative phase is in-phase, as in a bounding gait, the left and right limbs move simultaneously and the periodic trajectories are also almost identical between the left and right limbs. In contrast, during a galloping gait, the relative phase is not in-phase or antiphase as shown in Fig. 1**A** and the periodic trajectories differ between the left and right limbs, which leads to the difference in touchdown positions relative to the body as shown in Fig. 3 [21]. That is, the touchdown angles are different between the left and right limbs.

In our model, when we use identical touchdown angles between the left and right limbs ($\gamma_{\mathrm{LF}}^{\mathrm{TD}} = \gamma_{\mathrm{TF}}^{\mathrm{TD}}$, $\gamma_{\mathrm{LH}}^{\mathrm{TD}} = \gamma_{\mathrm{TH}}^{\mathrm{TD}}$), foot contact occurs simultaneously between the left and right limbs, which produces a bounding gait and a zero relative phase between the left and right limbs. In contrast, different touchdown angles ($\gamma_{\mathrm{LF}}^{\mathrm{TD}} \neq \gamma_{\mathrm{TF}}^{\mathrm{TD}}$, $\gamma_{\mathrm{LH}}^{\mathrm{TD}} \neq \gamma_{\mathrm{TH}}^{\mathrm{TD}}$) induce different foot contact timings and positions between the left and right limbs and yield a galloping gait. In addition, an increase in the touchdown angle difference indicates an increase in the relative phase between the left and right limbs.

2.4. Search of periodic solutions and stability analysis

We define the Poincaré section when $\dot{y}^* = 0$ and when all four limbs are in the swing phase (the model is in the flight phase). We find a periodic solution, which corresponds to a gait, by searching for a fixed point in the Poincaré section, where we neglect x^* because the horizontal position monotonically increases during locomotion. In addition, we assume that all four limbs have to experience the stance phase at least once before the intersection with the Poincaré section so that the solution explains a gait. When we set $z^* = [\, y^* \, \theta \, \dot{x}^* \, \dot{\theta}^* \,]^{\mathrm{T}}$, the Poincaré map P is written as

$$z^*_{n+1} = P(z^*_n, u^*) \tag{3}$$

where z^*_n is the value of z^* at the nth intersection with the Poincaré section and u^* is the parameter set. When we denote $\hat{z}^*$ for the fixed point on the Poincaré section, we obtain $\hat{z}^* = P(\hat{z}^*, u^*)$.

In this paper, because the left–right touchdown angle differences are not so different between the forelimbs and hindlimbs during galloping gaits [21], we find gaits in which the differences in the left and right touchdown angles are identical between the forelimbs and hindlimbs ($\gamma^{\mathrm{TD}}_{\mathrm{LF}} - \gamma^{\mathrm{TD}}_{\mathrm{TF}} = \gamma^{\mathrm{TD}}_{\mathrm{LH}} - \gamma^{\mathrm{TD}}_{\mathrm{TH}}$). In this condition, we can write the touchdown angles using the difference δ (≥ 0) by $\gamma^{\mathrm{TD}}_{\mathrm{LF}} = \bar{\gamma}^{\mathrm{TD}}_{\mathrm{F}} + \delta/2$, $\gamma^{\mathrm{TD}}_{\mathrm{TF}} = \bar{\gamma}^{\mathrm{TD}}_{\mathrm{F}} - \delta/2$, $\gamma^{\mathrm{TD}}_{\mathrm{LH}} = \bar{\gamma}^{\mathrm{TD}}_{\mathrm{H}} + \delta/2$, and $\gamma^{\mathrm{TD}}_{\mathrm{TH}} = \bar{\gamma}^{\mathrm{TD}}_{\mathrm{H}} - \delta/2$ ($\bar{\gamma}^{\mathrm{TD}}_{\mathrm{F}}, \bar{\gamma}^{\mathrm{TD}}_{\mathrm{H}} \geq 0$), and the parameter set of this model is given by $u^* = [\, I^* \, k^* \, l^* \, \bar{\gamma}^{\mathrm{TD}}_{\mathrm{F}} \, \bar{\gamma}^{\mathrm{TD}}_{\mathrm{H}} \, \delta \,]^{\mathrm{T}}$. We used the following four constraints: $\hat{y}^* = y^*_0$, $\hat{\theta} = \theta_0$, $\hat{\dot{\theta}}^* = \dot{\theta}^*_0$, and $Fr = Fr_0$, where Fr is the Froude number defined by

$$Fr = \left\{ \frac{1}{\tau^*} \int_0^{\tau^*} \dot{x}^* dt^* \right\}^2 \tag{4}$$

and τ^* is a dimensionless one gait cycle [1]. We determined $I^* = 0.1$ and $l^* = 0.6$ based on the physical parameters of such quadruped animals as horses, dogs, cheetahs, and goats [15, 20, 25, 39], and used $y^*_0 = 0.94$ and $\theta_0 = 0.018$. To clarify the dynamic characteristics of galloping gait of our model, we used various values for k^*, $\dot{\theta}_0^*$, and Fr_0 and searched $\hat{x}^*$, $\bar{\gamma}_{\mathrm{F}}^{\mathrm{TD}}$, $\bar{\gamma}_{\mathrm{H}}^{\mathrm{TD}}$, and δ that satisfy $\hat{z}^* = P(\hat{z}^*, u^*)$, where we used the fsolve function of MATLAB.

When we found periodic gaits, we investigated the local stability from the eigenvalues of the linearized Poincaré map around the fixed points. Because our model is energy conservative, the gait is asymptotically stable when all the eigenvalues except for one eigenvalue of 1 are inside the unit circle (these magnitudes are less than 1).

3. Results

We obtained various periodic gaits depending on Fr_0, k^*, and $\dot{\theta}_0^*$. Figures 4**A** and **B** show the angle difference δ for Fr_0 and k^* for the obtained gaits with $\dot{\theta}_0^* = 0.92$ and 1.65, respectively. The gray regions show unstable gaits and the white regions show stable gaits. The obtained gaits have different sequences of the stance status (Sequences A–E), depending on the parameters, as shown in Fig. 5. The obtained gaits in Fig. 4**A** have Sequences A–E, whereas those in Fig. 4**B** have only Sequence E. Sequences B and E correspond to the transverse and rotary gallops, respectively, in Fig. 1**B**. In both Figs. 4**A** and **B**, as the locomotion speed increases, δ decreases and approaches 0 (but, did not reach 0). At slow speeds (small Froude number), the obtained gaits are unstable, and when the locomotion speed increases, the gaits become stable. The dimensionless spring stiffness was estimated as 7 [14] or 12 [27] for horses, 11 [14] for dogs, and 16 [14] for goats. The left–right touchdown angle difference during galloping gaits was observed around 5 to 15° [21]. The Froude number of various quadruped animals is shown in Fig. 1**A** and about 3 during the transverse gallop of goats [14], and is seen to be greater than 50 during the rotary galloping of cheetahs [5]. Our simulation results are comparable with biological data.

To evaluate the biological relevance of the obtained gaits, we compared the vertical COM movement of our simulation results with data measured during quadrupedal galloping gaits. In Fig. 6**A**, we used $\dot{\theta}_0^* = 0.92$, $Fr_0 = 14.4$,

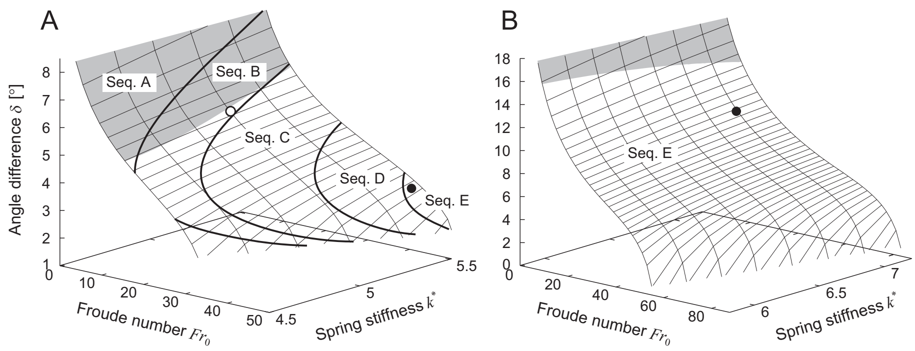

Figure 4: Touchdown angle difference δ of obtained gaits for Froude number Fr_0 and spring stiffness k^* with (**A**) $\dot{\theta}_0^* = 0.92$ and (**B**) $\dot{\theta}_0^* = 1.65$. Gray regions show unstable gaits, and white regions show stable gaits. **A** has five gaits (Sequences (Seqs.) A–E) depending on Fr_0 and k^*, while **B** has one gait (Sequence E). Sequences A–E have different sequences of the stance condition, as shown in Fig. 5. The open dot (in **A**) and the black dots (in **A** and **B**) are the parameter sets used in Fig. 6 to compare vertical COM movement with the measured data for transverse and rotary gallops, respectively.

and $k^* = 5.1$ (open dot in Fig. 4**A**) and compared the simulation result with data measured during a transverse gallop by a horse (the Froude number is around 18) [34]. The simulation result shows a single sinusoidal curve, and the magnitude is similar to that of the measured data. The dimensionless spring stiffness of a horse transverse gallop was estimated by 12 [27], and the simulation result is fairly consistent with the measured data. In Fig. 6**B**, we used $\dot{\theta}_0^* = 0.92$, $Fr_0 = 42.1$, and $k^* = 5.5$ (black dot in Fig. 4**A**) and $\dot{\theta}_0^* = 1.65$, $Fr_0 = 25.7$, and $k^* = 7.0$ (black dot in Fig. 4**B**) and compared these simulation results with data measured during a rotary gallop by a dog (the Froude number is about 20) [4]. The dimensionless spring stiffness of dogs was estimated by 11 [14]. When $\dot{\theta}_0^* = 0.92$, the simulation result is very different in shape and magnitude from the measured data. In contrast, for $\dot{\theta}_0^* = 1.65$, although the magnitude is slightly lower than the measured data, the simulation result shows a double sinusoidal curve and has a similar shape to the measured data. This simulation result is consistent with the measured data. See supplementary movies in Appendix A for simulated locomotor behaviors.

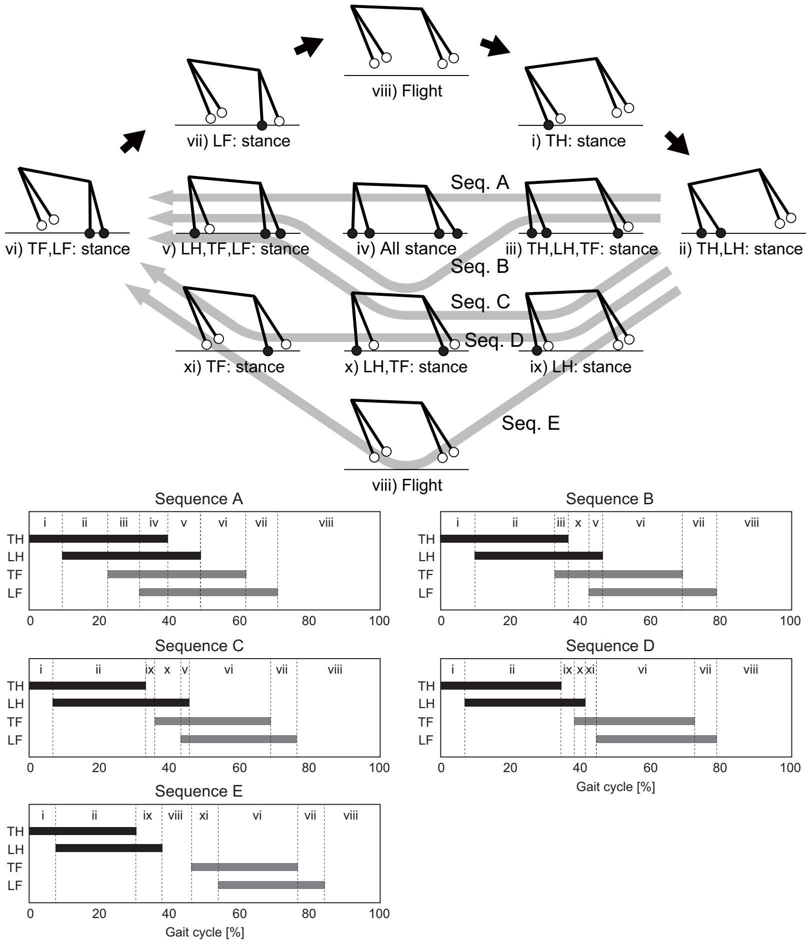

Figure 5: Schematic sequences of stance condition of obtained gaits: Sequences (Seqs.) A–E. TH: trailing hindlimb, TF: trailing forelimb, LH: leading hindlimb, and LF: leading forelimb.

To clarify the dynamical difference between the obtained transverse and rotary gallops, we investigated the energy transfer during one gait cycle. Figures 7**A** and **B** show the ratio of four components of the conservative mechanical energy (the gravitational energy (zero at the bottom of the vertical COM movement), forelimb and hindlimb spring energies, and kinetic energy) for $\dot{\theta}_0^* = 0.92$, $Fr_0 = 14.4$, and $k^* = 5.1$ (transverse gallop), and $\dot{\theta}_0^* = 1.65$, $Fr_0 = 25.7$, and $k^* = 7.0$ (rotary gallop), respectively. In the transverse gallop, the gravitational and kinetic energies move to the hindlimb spring energy during the first half

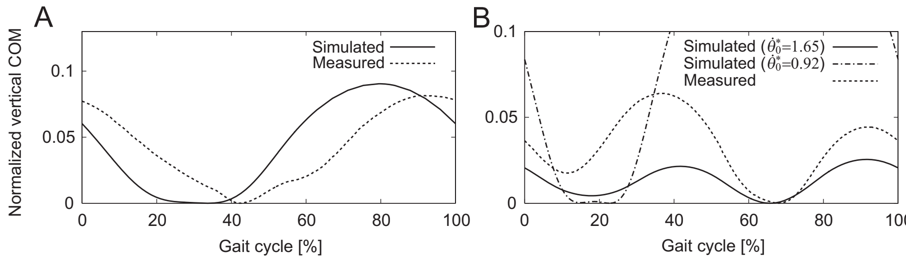

Figure 6: Comparison of vertical COM movement between the simulation results and measured data for one gait cycle between touchdowns of trailing hindlimbs during quadrupedal galloping gaits. **A**: transverse gallop using $\dot{\theta}_0^* = 0.92$, $Fr_0 = 14.4$, and $k^* = 5.1$. Measured data are based on [34] from a horse. **B**: rotary gallop using $\dot{\theta}_0^* = 0.92$, $Fr_0 = 42.1$, and $k^* = 5.5$ and $\dot{\theta}_0^* = 1.65$, $Fr_0 = 25.7$, and $k^* = 7.0$. Measured data are based on [4] from a dog.

of the hindlimb stance phase. The energy transitions into the kinetic energy during the last half of the stance phase, and then changes to the forelimb spring energy due to the touchdown of the forelimbs. Finally, it moves back to the gravitational and kinetic energies. In the rotary gallop, the gravitational and kinetic energies transition into the hindlimb spring energy during the first half of the hindlimb stance phase, similarly to the transverse gallop. However, the energy returns to the gravitational and kinetic energies during the last half of the stance phase unlike the transverse gallop. The similar energy transfer occurs in the forelimb stance phase. Although the rotary gallop has the energy transfer to the gravitational energy between the hindlimb and forelimb stance phases, the transverse gallop does not have such an energy transfer. This difference produces two types of galloping gaits; the transverse gallop with a single flight phase and the rotary gallop with two flight phases.

4. Discussion

In this paper, we produced galloping gaits using a simple model with a rigid body and four massless springs, and showed that the model can explain specific characteristics in a quadrupedal galloping gait, such as dependence of left–right

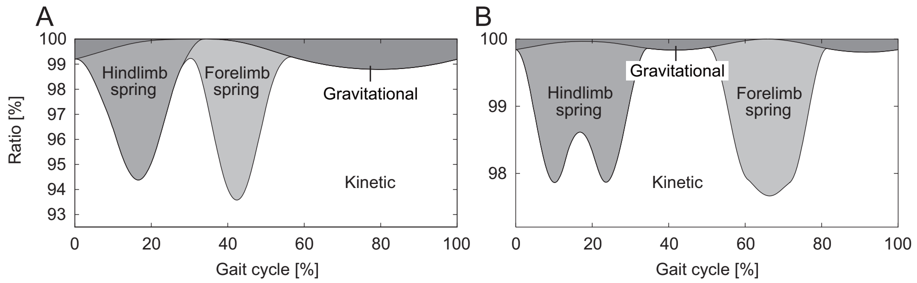

Figure 7: Energy transfer during one gait cycle for (**A**) transverse gallop using $\dot{\theta}_0^* = 0.92$, $Fr_0 = 14.4$, and $k^* = 5.1$ and (**B**) rotary gallop using $\dot{\theta}_0^* = 1.65$, $Fr_0 = 25.7$, and $k^* = 7.0$.

asymmetry in gait parameters on the locomotion speed, from the viewpoint of dynamics.

4.1. Asymmetric gait parameters

In quadrupedal galloping gaits, the relative phase between the left and right limbs is away from the antiphase, irrespective of species, as shown in Fig. 1**A** [1]. In addition, the relative phase decreases and approaches in-phase as the locomotion speed increases; however, it does not reach complete in-phase. These characteristics reflect the left–right asymmetry in touchdown angles, as shown in Fig. 3 [21]. We focused on this asymmetry to produce the galloping gait of our model. As the locomotion speed increased, the left–right touchdown angle difference decreased and approached 0 (but did not reach 0), as shown in Fig. 4. This means that the relative phase difference decreased and approached in-phase. This trend is consistent with the observations in quadrupedal galloping gaits. Furthermore, the fact that there is no solution for the zero left–right touchdown angle difference means that this asymmetry in touchdown angles allows the model to produce periodic solutions for gaits, which may suggest an important role of left–right asymmetry in touchdown angles in the locomotion dynamics of galloping gaits.

4.2. Transverse and rotary gallops

There are basically two types of galloping gaits (transverse and rotary gallops) in quadruped animals, and they have different footfall sequences as shown in Fig. 1**B**. The transverse gallop observed often in horses has a single flight phase after the liftoff of the forelimbs. In contrast, the fast rotary gallop observed often in dogs and cheetahs has another flight phase after the liftoff of the hindlimbs in addition to the flight phase after the liftoff of the forelimbs. Our simulation results showed that our model produced various galloping gaits depending on the parameters, which had different sequences of the stance condition (Sequences A–E), as shown in Fig. 5. As locomotion speed and spring stiffness increased, the sequence of the stance condition changed from Sequence A to E. Sequences B and E corresponded to the transverse and rotary gallops, respectively (because we cannot determine left and right limbs due to the two-dimensional nature of our model, we decided these gaits from the number of flight phases). However, even when the sequences of the stance condition were identical, the locomotor behavior of the obtained gaits, such as the vertical COM movement, differed depending on the parameters, as shown in Fig. 6. Depending on the model parameters, both the sequences of stance condition and locomotor behavior of the obtained gaits were comparable to those in quadruped animals, which was evaluated by comparing our simulation results with measured data of quadruped animals. Although quadruped animals use these two different gaits depending on the locomotion speed and species, our simple model can explain these different gaits using only a few parameters.

The transverse gallop has a small relative phase between the forelimbs and hindlimbs, while the rotary gallop has a large relative phase, as shown in Fig. 1**B**. In our simulation results, different parameters produced different relative phase between the forelimbs and hindlimbs, as shown in Fig. 5, which changed the number of flight phases and induced different galloping gaits. While the relative phase between the left and right limbs depends on the left–right touchdown angle difference δ, our modeling has no constraint on the relative phase between the forelimbs and hindlimbs, which were only determined through gait dynamics with parameters. The dynamic mechanism that creates two different gaits was ascertained from the energy transfer during one gait cycle in Fig. 7. It has been suggested that horse transverse galloping and human skipping gaits have a similarity in the energy transfer between the leading and trailing limbs [30]. We also intend to investigate the mechanism by improving our model in the future.

4.3. Gait stability

Gait stability is an important factor in dynamic locomotion, as investigated in humans [17, 19, 38] and quadrupeds [2, 3, 10, 12, 35, 37]. Our simulation results showed that the galloping gait of our model was stable depending on the Froude number (Fig. 4). That is, our model had self-stability for a particular locomotion speed. More specifically, our model generated stable galloping gaits only at fast locomotion speeds ($Fr_0 > 5$), which is consistent with the observation in quadrupedal galloping gaits as shown in Fig. 1**A** [1]. At slow speeds, the obtained galloping gaits became unstable. This limitation of gait stability due to the decrease in locomotion speed suggests a change of the gait to an alternative gait, such as a trotting gait, to improve gait stability.

4.4. Limitation of our model and future work

In this study, we used a very simplified physical model for quadrupedal galloping gaits. For example, the galloping quadruped animal was modeled by a single rigid body and four massless springs, and symmetric assumptions between the forelimbs and hindlimbs were used in the model parameters, such as the left–right touchdown angle difference δ and dimensionless spring stiffness k^*. Such simplifications resulted in quantitative differences in locomotion parameters from actual animals. However, it is clear that our model showed similar trends in the asymmetric gait parameters for the locomotion speed and in the generation of two different galloping gaits, which are characteristic for quadrupedal galloping gaits, as was confirmed by the comparisons with quadruped animals. This suggests that our simple model is capable of capturing the essential aspects needed to generate the galloping gait in quadruped animals from the viewpoint of dynamics. To further clarify the underlying mechanisms in quadrupedal galloping gaits, we intend to develop a more sophisticated and plausible model by incorporating important dynamical factors, such as muscle actuators, frictional dissipation, and neuromechanical interactions, in future studies.

Appendix A. Supplementary materials

We prepared two supplementary movies on the transverse and rotary gallops obtained in our simulation:

1. Transverse gallop using $\dot{\theta}_0^* = 0.92$, $Fr_0 = 14.4$, and $k^* = 5.1$.
2. Rotary gallop using $\dot{\theta}_0^* = 1.65$, $Fr_0 = 25.7$, and $k^* = 7.0$.

Acknowledgment

This paper was supported in part by JST, CREST.

Conflict of interest statement

The authors have no conflict of interests.

References

[1] Alexander, R.McN., and Jayes, A.S., 1983. *A dynamic similarity hypothesis for the gaits of quadrupedal mammals*, J. Zool., Lond., 201:135–152.

[2] Aoi, S., Yamashita, T., and Tsuchiya, K., 2011. *Hysteresis in the gait transition of a quadruped investigated using simple body mechanical and oscillator network models*, Phys. Rev. E, 83(6):061909.

[3] Aoi, S., Katayama, D., Fujiki, S., Tomita, N., Funato, T., Yamashita, T., Senda, K., and Tsuchiya, K., 2013. *A stability-based mechanism for hysteresis in the walk–trot transition in quadruped locomotion*, J. R. Soc. Interface, 10(81):20120908.

[4] Bertram, J.E.A. and Gutmann, A., 2009. *Motions of the running horse and cheetah revisited: fundamental mechanics of the transverse and rotary gallop*, J. R. Soc. Interface, 6:549–559.

[5] Biancardi, C.M. and Minetti, A.E., 2012. *Biomechanical determinants of transverse and rotary gallop in cursorial mammals*, J. Exp. Biol., 215:4144–4156.

[6] Blickhan, R., 1989. *The spring–mass model for running and hopping*, J. Biomech., 22:1217–1227.

[7] Bullimore, S.R. and Burn, J.F., 2006. *Dynamically similar locomotion in horses*, J. Exp. Biol., 209:455-465.

[8] Bullimore, S.R. and Burn, J.F., 2006. *Consequences of forward translation of the point of force application for the mechanics of running*, J. Theor. Biol., 238:211-219.

[9] Bullimore, S.R. and Burn, J.F., 2007. *Ability of the planar spring-mass model to predict mechanical parameters in running humans*, J. Theor. Biol., 248:686-695.

[10] Cao, Q. and Poulakakis, I., 2013. *Quadrupedal bounding with a segmented flexible torso: passive stability and feedback control*, Bioinspir. Biomim., 8:046007.

[11] Cavagna, G.A., Heglund, N.C., and Taylor, C.R., 1977. *Mechanical work in terrestrial locomotion: two basic mechanisms for minimizing energy expenditure*, Am. J. Physiol., 233(5):R243–R261.

[12] Diedrich, F.J. and Warren Jr., W.H., 1998. *Why change gaits? Dynamics of the walk-run transition*, J. Exp. Psychol. Hum. Percept. Perform., 21:183–202.

[13] Farley, C.T. and Taylor, C.R., 1991. *A mechanical trigger for the trot-gallop transition in horses*, Science, 253:306–308.

[14] Farley, C.T., Glasheen, J., and McMahon, T.A., 1993. *Running springs: Speed and animal size*, J. Exp. Biol., 185:71–86.

[15] Fischer, M.S., Lilje, K.E., Lauströer, J., and Andikfar, A., 2011. Dogs in motion, *Dortmund: VDH-Service GmbH.*

[16] Full, R.J. and Koditschek, D.E., 1999. *Templates and anchors: neuromechanical hypotheses of legged locomotion on land*, J. Exp. Biol., 202:3325–3332.

[17] Geyer, H., Seyfarth, A., and Blickhan, R., 2005. *Spring-mass running: simple approximate solution and application to gait stability*, J. Theor. Biol., 232:315–328.

[18] Geyer H., Seyfarth, A., and Blickhan, R., 2006. *Compliant leg behaviour explains basic dynamics of walking and running*, Proc. R. Soc. B, 273:2861–2867.

[19] Ghigliazza, R.M., Altendorfer, R., Holmes, P., and Koditschek, D., 2003. *A simply stabilized running model*, SIAM J. Appl. Dyn. Syst., 2(2):187–218.

[20] Grossi, B. and Canals, M., 2010. *Comparison of the morphology of the limbs of juvenile and adult horses (Equus caballus) and their implications on the locomotor biomechanics*, J. Exp. Zool., 313A:292–300.

[21] Herr, H.M. and McMahon, T.A., 2001. *A galloping horse model*, Int. J. Robot. Res., 20(1):26–37.

[22] Hildebrand, M., 1977. *Analysis of asymmetrical gaits*, J. Mammal., 58(2):131–156.

[23] Hildebrand, M., 1989. *The quadrupedal gaits of vertebrates*, BioScience, 39(11):766–775.

[24] Hoyt, D.F. and Taylor, C.R., 1981. *Gait and the energetics of locomotion in horses*, Nature, 292:239–240.

[25] Hudson, P.E., Corr, S.A., and Wilson, A.M., 2012. *High speed galloping in the cheetah (Acinonyx jubatus) and the racing greyhound (Canis familiaris): spatio-temporal and kinetic characteristics*, J. Exp. Biol., 215:2425–2434.

[26] Marhefka, D.W., Orin, D.E., Schmiedeler, J.P., and Waldron, K.J., 2003. *Intelligent control of quadruped gallops*, IEEE/ASME Trans. Mechatron., 8(4):446–456.

[27] McGuigan, M.P. and Wilson, A.M., 2003. *The effect of gait and digital flexor muscle activation on limb compliance in the forelimb of the horse Equus caballus*, J. Exp. Biol., 206:1325–1336.

[28] McMahon, T.A., 1985. *The role of compliance in mammalian running gaits*, J. Exp. Biol., 115:263–282.

[29] McMahon, T.A. and Cheng, G.C., 1990. *The mechanics of running: how does stiffness couple with speed?*, J. Biomech., 23(Suppl. 1):65–78.

[30] Minetti, A.E., 1998. *The biomechanics of skipping gaits: a third locomotion paradigm?*, Proc. R. Soc. Lond. B, 265:1227–1235.

[31] Minetti, A.E., Ardigo, L.P., Reinach, E., and Saibene, F., 1999. *The relationship between mechanical work and energy expenditure of locomotion in horses*, J. Exp. Biol., 202:2329–2338.

[32] Muybridge, E., 1957. Animals in motion, *New York: Dover Publications.*

[33] Nanua, P. and Waldron, K., 1995. *Energy comparison between trot, bound, and gallop using a simple model*, ASME J. Biomech. Eng., 117:466–473.

[34] Pfau, T., Witte, T.H., and Wilson, A.M., 2006. *Centre of mass movement and mechanical energy fluctuation during gallop locomotion in the Thoroughbred racehorse*, J. Exp. Biol., 209:3742–3757.

[35] Poulakakis, I., Papadopoulos, E., and Buehler, M., 2006. *On the stability of the passive dynamics of quadrupedal running with a bounding gait*, Int. J. Robot. Res., 25(7):669–687.

[36] Raibert, M.H., 1986. Legged robots that balance, *Cambridge: MIT Press.*

[37] Schöner, G., Jiang, W.Y., and Kelso, J.A.S., 1990. *A synergetic theory of quadrupedal gaits and gait transitions*, J. Theor. Biol., 142:359–391.

[38] Seyfarth, A., Geyer, H., Günther, M., and Blickhan, R., 2002. *A movement criterion for running*, J. Biomech., 35:649–655.

[39] Taylor, C.R., Shkolnik, A., Dmi'el, R., Baharav, D., and Borut, A., 1974. *Running in cheetahs, gazelles, and goats: energy cost and limb conjguration*, Am. J. Physiol., 227(4):848–850.

[40] Waldron, K., Estremera, J., Csonka, P., and Singh, S., 2009. *Analyzing bounding and galloping using simple models*, ASME J. Mech. Rob., 1(1):011002.